Effect of the semi-conductive properties of the passive layer on the current provided by stainless steel microbial cathodes

Liz Pons, Marie-Line Délia, Régine Basséguy, Alain Bergel*

Laboratoire de Génie Chimique, CNRS – Université de Toulouse, 4 allée Emile Monso BP 84234, 31030 Toulouse, France

A B S T R A C T

Geobacter sulfurreducens biofilms were formed under constant polarisation at −0.6 V vs. Ag/AgCl on stainless steel cathodes to catalyse the reduction of fumarate. The time-evolution of the current strongly depended on the quality of the inoculum. Inoculating with young cells significantly shortened the initial lag-phase and using the same inoculum improved the reproducibility of the current–time curves. The whole set of experiments showed that 254SMO stainless steel provided higher current densities (on average 14.1 A/m^2) than biofilms formed on 316L stainless steel (on average 4.5 A/m^2). Biofilm coverage assessed by epifluorescent microscopy showed that coverage ratios were generally higher for 316L than for 254SMO. It must be concluded that 254SMO is more efficient in transferring electrons to bacterial cells than 316L. Mott–Schottky diagrams recorded on both materials under conditions of electrolysis in the absence of microorganisms showed that the surface oxide layers had similar n-type semi-conductive behaviour for potential values higher than the flat band potential. In contrast, 316L exhibited slight p-type behaviour at potential lower than the flat band potential, while 254SMO did not. The higher electrochemical performances of biocathodes formed on 254SMO are explained by semi-conductive properties of its passive layer, which prevented the p-type behaviour occurring in cathodic electrolysis conditions.

1. Introduction

The capacity of microbial biofilms to catalyse electrochemical reactions was discovered recently [1,2] and has led to the exponential development of a new thematic area over the past few years. The electrochemistry of microbial biofilms has been investigated mainly in the aim of developing microbial fuel cells (MFC) [3–6]. Most studies in this field have dealt with the catalysis of anode reactions; fewer have been devoted to the catalysis of cathode reactions [7–9] even though the cathode process remains a crucial problem for MFC development. The concept of electro-active biofilms may also lead to novel processes outside the field of fuel cells, for instance in the design of biosensors [10], for soil remediation by biofilm-catalysed electrolysis or dechlorination processes [5,11,12]. Currently, the main successes for biofilm-catalysed electrolysis have been obtained for the production of hydrogen in so-called microbial electrolysis cells (MEC) [13–16]. In this framework, biofilms have generally been used to oxidise organic compounds at the anode but biofilms have also been implemented recently on the cathode for the catalysis of hydrogen release [17]. Biofilms formed from pure culture of *Geobacter sulfurreducens* have been shown to be able to form efficient biocathodes reducing fumarate to succinate [18]:

$$\text{Fumarate} + 2H^+ + 2e^- \rightarrow \text{Succinate} \quad (1)$$

Maximum current densities of 0.4 A/m^2 [18] and 0.75 A/m^2 [19] have been obtained on graphite electrodes polarised at −0.5 V and −0.6 V vs. Ag/AgCl respectively, but our previous work has demonstrated that much higher values are provided when the graphite cathode is replaced by stainless steel. Up to 20.5 A.m^2 was thus sustained under polarisation at −0.6 V vs. Ag/AgCl [19]. The increase in current density of more than one order of magnitude gained by using stainless steel instead of graphite, in exactly identical conditions, highlights the great interest of understanding the electron transfer mechanisms on stainless steel. With regard to the high current density obtained biofilm-covered stainless steel cathodes are becoming very interesting tools for designing microbial-catalysed electro-synthesis. Such microbial biocathodes could provide promising alternative routes to the numerous bio-electro-synthesis pathways that have been investigated so far with the association between electrodes and enzymes [20]. Microbial cathodes should allow enzyme catalysis to be used without extracting the enzymes from the cells and consequently avoiding all the cumbersome steps of enzyme extraction, purification and immobilization on the electrode surface.

* Corresponding author. Tel.: +33 05 3432 3673; fax: +33 05 3432 3600.
E-mail address: alain.bergel@ensiacet.fr (A. Bergel).

The purpose of the work presented here was to progress in understanding the kinetics of *G. sulfurreducens* biofilm-coated stainless steel cathodes. It is known in the field of microbial corrosion that the chemical composition of stainless steels has a strong effect on their electrochemical behaviour and on microbial adhesion to their surface [21,22]. Recent studies have revealed significant differences in the efficiency of austenitic (304L) and superaustenitic (254SMO) steels for oxygen reduction in natural [23] or artificial seawater [24]. The differences observed on the kinetics of oxygen reduction have been attributed to the semiconductive properties of their passive layer, which have been characterised by the Mott–Schottky technique. These previous studies, which were aimed at understanding corrosion mechanisms, were performed in aerobic environments and most often with material kept at open circuit. A similar approach was used here but adapted to the electrolysis conditions, i.e. under constant polarisation and in anaerobic medium, with the view to optimising *G. sulfurreducens* microbial stainless steel cathodes.

2. Experimental

2.1. Media and growth conditions

Geobacter sulfurreducens strain PCA (ATCC51573) was purchased from DSMZ (Deutsche Sammlung von Mikroorganismen und Zellkulturen). The growth medium contained per litre: 0.1 g KCl, 1.5 g NH_4Cl, 2.5 g $NaHCO_3$, 0.6 g NaH_2PO_4, 0.82 g sodium acetate, 8 g sodium fumarate, 10 mL Wolfe's vitamin solution (ATCC MD-VS) stored at −20 °C and 10 mL modified Wolfe's minerals (ATCC MD-TMS) stored at 4 °C. The medium without sodium fumarate, vitamins and minerals was first sterilised in bottles. After sterilisation, the medium was completed with the filtered (0.2 μm) stock solution of sodium fumarate to get the complete growth medium. *G. sulfurreducens* cells were grown following two different procedures. In the "one-step procedure", *G. sulfurreducens* (10%, v/v, from an inoculum stored at −20 °C) was incubated at 30 °C for the time required (generally 90–100 h) to obtain a final optical density of 0.4 at 620 nm, corresponding to a microbial concentration of around 189,000 colony forming units per mL (CFU mL^{-1}) [19]. This solution was used to inoculate the electrochemical reactors. In some cases the culture was implemented following two successive steps ("two-step procedure") in order to control the physiological state of the cells. *G. sulfurreducens* (10%, v/v, from an inoculum stored at −20 °C) was incubated at 30 °C for 80 h in the growth medium to a final optical density of 0.3 at 620 nm. For the second culture step, 5 mL of the suspension was inoculated into 45 mL of the same medium. The second incubation lasted 38 h to obtain the final optical density of 0.4 at 620 nm.

2.2. Electrodes and electrochemical reactors

Stainless steel electrodes were made of austenitic stainless steel UNS S31603 (AISI 316L, 2.5 cm × 2.5 cm × 0.1 cm) composition (0.019% C, 17.3% Cr, 2.04% Mo, 11.3% Ni, 1.04% Mn, 0.041% N), and superaustenitic stainless steel UNS S31254 (254SMO, 1.0 cm × 2.5 cm × 0.1 cm) composition (0.01% C, 19.9% Cr, 6% Mo, 17.8% Ni, 0.5% Mn, 0.02% N). They were cleaned for 20 min with 50–50% ethanol/acetone, then for 15 min with 2–20% fluoridric–nitric solution and rinsed with water. One face was coated with insulating resin (Resipoly Chrysor) so that current came only from the face that was being tested for microbial adhesion.

Electrochemical experiments were carried out in 0.5 L electrochemical reactors containing 0.45 L culture medium without acetate (electron donor). The reactors were continuously flushed with N_2–CO_2 (80–20%). Bacteria were injected into the reactors (10% v/v) after 12 h. The working electrodes were polarised with a multi-potentiostat (VMP-Biologic) vs. a silver/silver chloride electrode (Ag/AgCl) constituted of a silver wire coated by silver chloride, those potential in the culture medium was 0.313 V vs. SHE. The potential of the Ag/AgCl electrodes was checked at the beginning and the end of experiments with respect to a SCE to verify its stability. The auxiliary electrode was a platinum grid. Cyclic voltammetry (CV) was performed at 10 mV/s in the range −0.6 to 0.3 V vs. Ag/AgCl at the beginning (before inoculation) and at the end of the experiment.

2.3. Microscopy and statistical analysis

At the end of the experiments, the electrodes were stained with 0.03% acridine orange (A6014, Sigma) for 10 min, rinsed with normal saline (9% NaCl) and air dried. Microscopy was performed using a Carl Zeiss Axiotech 100 microscope equipped for epifluorescence with an HBO 50/ac mercury light source and a Zeiss 09 filter. Images were taken with a monochrome digital camera (Evolution VF). Each picture, which had an area of around 5200 μm^2, was processed with the Image-Pro-Plus V5 software to calculate the percentage of surface covered by bacteria (θ). For each electrode, the same calculation was done on 40 pictures taken at different locations to extract an average coverage ratio (θ_A) that assessed the global coverage of bacteria on the electrode surface. The relative error was calculated using a Student test ($P = 0.95$).

2.4. Mott–Schottky diagrams

Mott–Schottky diagrams were plotted at a frequency of 1502 Hz, with 10 mV amplitude. This amplitude was within the range of linearity checked by oscilloscope measurements. Potentials were swept from −1.5 V to +0.5 V vs. Ag/AgCl in steps of 50 mV every 0.1 s. The capacitance of the passive layer was calculated from the Mott–Schottky equation:

$$C_{SC}^{-2} = \frac{2}{e\varepsilon\varepsilon_0 N_q S^2}\left(U_{fb} - E - \frac{k_B T}{e}\right) \quad \text{(I)}$$

where C_{SC} is the capacitance of the semi-conductive passive layer, ε is the permittivity of the passive layer, which was fixed at the commonly used value of 12 [24], ε_0 is the vacuum permittivity (8.8542×10^{-14} F cm^{-1}), N_q is the charge carrier density, U_{fb} is the flat band potential, E is the applied potential, S is the surface area in contact with the electrolyte and k_B is the Boltzmann constant (1.3806×10^{-23} J K^{-1}). The thickness of the space charge region, W, was calculated according to

$$W = \frac{\varepsilon\varepsilon_0}{C(\max)} \quad \text{(II)}$$

where $C(\max)$ is the capacitance corresponding to the maximum obtained by plotting C^{-2} as a function of E.

3. Results and discussion

3.1. Effect of inoculum preparation on current evolution

Geobacter sulfurreducens cells were grown in their traditional culture medium following a common one-step procedure (see Section 2) and the culture was used as inoculum just after the single incubation step. The electrochemical reactors contained the culture medium without acetate (electron donor) to force the bacterial cells to use the cathode as the electron source for the reduction of fumarate to succinate (reaction (1)). Electrodes were polarised at −0.6 V vs. Ag/AgCl so that the initial current was very close to zero. After 12 h, the reactors were inoculated with 10% v/v of the bacterial culture. The general variation of the current with time was always

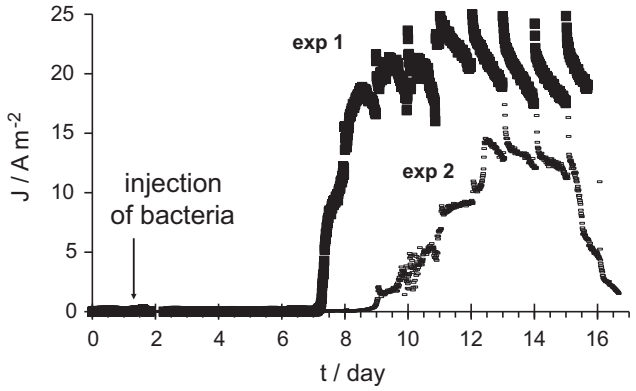

Fig. 1. Variation of the current density on 254SMO (■) cathode polarised at −0.6 V vs. Ag/AgCl with two different inoculum produced by one-step incubation (experiments 1 and 2 reported in Table 1). Sharp current variations corresponded to periodic voltammetry records.

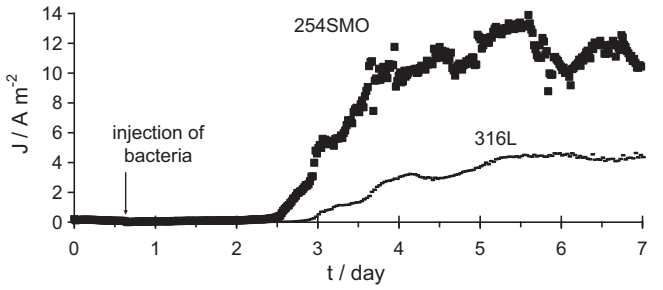

Fig. 2. Variation of the current density on 316L (-) and 254SMO (■) cathode polarised at −0.6 V vs. Ag/AgCl obtained with parallel experiments using the same inoculum produced by two-step incubation (experiments 11 and 12 reported in Table 1).

the same (Fig. 1): an initial lag-time followed by a sigmoid increase led, after a few days, to a current plateau that gave the maximal current density value (J_{max}). The maximum value remained roughly stable for several days, with circadian oscillation due to temperature variation [25]. Such a shape is commonly attributed to the control of the current by formation of an electro-active biofilm on the electrode surface [18,19].

Six independent experiments were performed with 254SMO cathodes (no. 1–6 in Table 1) each time with a new inoculum. Maximal current densities varied from 12 to 20 A/m^2 and the time required to reach these maximal values was very different from one experiment to another. Particularly, the initial lag-phase times varied a lot, as emphasised in Fig. 1. The electrochemical activity of the biofilms and the kinetics of its formation were very sensitive to the inoculum. A recent study that specifically dealt with the reproducibility of microbial fuel cell performances has put in light the very poor reproducibility of the results [26]. Here it was showed that even with pure culture and in electrochemical well-controlled conditions the reproducibility of the results remains poor when inocula coming from different incubations are used.

Further experiments were done by preparing the inoculum following a two-step procedure, which consisted in a first incubation of the *G. sulfurreducens* cells, which was stopped just at the end of the exponential growing phase and used as inoculum for the second incubation. Such a procedure is commonly used in biotechnology to better control the physiologic state of the cells, and particularly to mitigate the discrepancies due to the primary culture performed just after storage. Eight independent experiments were performed in such a way, four with 316L and four with 254SMO cathodes. The two-step procedure had statistically an important effect on the kinetic of the phenomenon, significantly reducing the initial lag phase to around 2 days (Fig. 2). This initial phase, which is controlled by cell adhesion and the first step of biofilm formation, is logically depending on the physiological state of the cells contained in the inoculum. The one-step procedure provided inocula that were produced by long-time incubation (around 90–100 h) resulting in long and poorly reproducible lag phases. The two-step procedure that provided younger inocula (the second incubation lasted less than 40 h) shortened the lag phase and made it reproducible to around 2 days (Fig. 2). Clearly younger cells were more suitable for fast adhesion and fast biofilm development.

Finally, experiment no. 11–14 were performed in parallel, exactly at the same time, in separated reactors and with the same inoculum that was produced by the two-step procedure. The three experiments performed with 254SMO electrodes (experiments 12–14 in Table 1) gave identical current evolution and even the experiment performed with 316L showed a similar short lag period of 2 days (Fig. 2 and Table 1). Experiments 12 and 13 were stopped at day 7, when the electrodes supplied 13 and 14 A/m^2 respectively.

Table 1
Maximal current density (J_{max}) and average biofilm coverage ratio (θ_A) obtained by chronoamperometry at −0.6 V vs. Ag/AgCl. The values of the coverage ratios were averaged from 40 pictures taken at different locations on the electrode surface. The relative error was calculated using a Student test ($P = 0.95$). Experiments 11 and 12, and 13 and 14, were done in parallel with the same inoculum produced by the two-step culture procedure.

No.	J_{max} (A/m^2)	Average coverage, θ_A (%)	Relative error on θ_A (%)	Time[a] (days)	Number of steps[b]
316L					
8	1	52	7	28	2
9	4	9.3	1.8	10	2
10	9	30	6	7	2
11[c]	4	9	2	7	2
254SMO					
1	20	6	3	17	1
2	15	9	5	17	1
3	17	3.6	2	20	1
4	12	14.7	4	20	1
5	13	1.6	1	20	1
6	17	14.6	5	20	1
7	11	39	7	9	2
12[c]	13	8	1.7	7	2
13[c]	14	5.2	1.1	7	2
14[c]	9	13.1	5.4	11	2

[a] Time from the injection of the inoculum i.e. biofilm age.
[b] Number of incubation steps performed for the preparation of the inoculum.
[c] Experiments performed in parallel at the same time with the same inoculum.

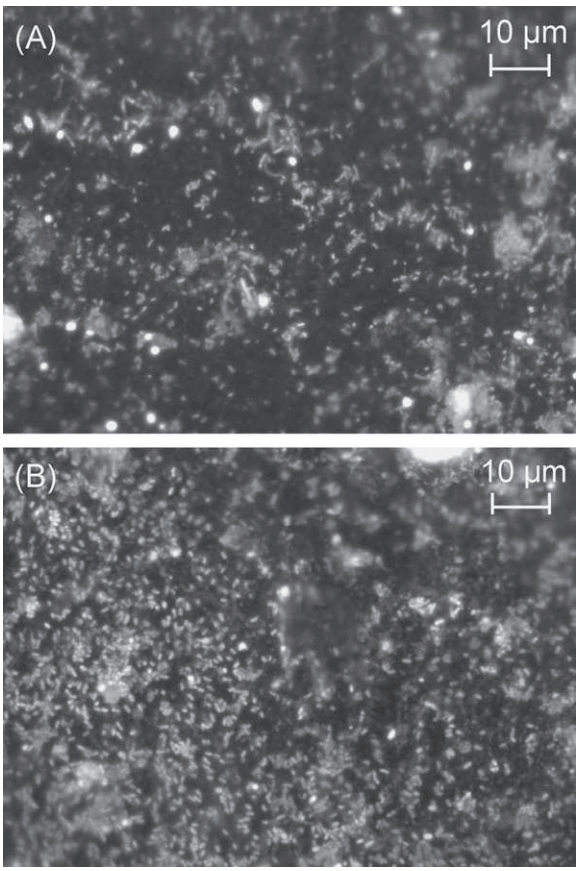

Fig. 3. Epifluorescence microscopy pictures of *G. sulfurreducens* biofilm on 254SMO (A) and 316L (B) electrode polarised at −0.6 V vs. Ag/AgCl for 9 and 7 days respectively (experiments 7 and 9 reported in Table 1). The coverage ratios on these spots were 14% and 49% respectively.

Experiment 14 was stopped four days later, when current density decreased to 9 A/m^2, but the three experiments showed exactly the same evolution during the first seven days. Implementing a two-step procedure and working in parallel with the same inoculum significantly improved the reproducibility of the electro-activity establishment.

3.2. Maximum current density and biofilm coverage on 316L and 254SMO electrodes

At the end of polarisation, the surface of each electrode was examined by epifluorescent microscopy. Biofilms always exhibited a very inhomogeneous structure. The microbial coating was mainly constituted of single adhered cells or of small microbial colonies scattered on the electrode surface. The heterogeneity of the coating led us to use a statistical approach to assess biofilm coverage. For each electrode, the images obtained on 40 different plots were numerically processed to determine the percentage of surface covered by the biofilm (Fig. 3). The overall biofilm coverage ratio (θ_A) of the electrode was assessed by averaging these 40 values (Table 1).

The first 6 independent experiments performed with 254SMO cathodes (no. 1–6 in Table 1) gave maximal current densities from 12 to 20 A/m^2 with disperse coverage ratios from 1.6 to 14.7% even with biofilms of the same age. Moreover, biofilm coverage measures done after 17 days and 20 days did not show a relation between the biofilm age and the coverage ratio. The current density provided by the electrodes revealed not to be straightforwardly depending on the biofilm coverage ratio, low currents can be obtained with high coverage, and inversely. The inoculum that was different for each experiment was the main parameter that controlled the electrochemical characteristics of the biofilm. The experiments conducted with the two-step prepared inocula confirmed that the maximum current provided by the electrodes does not depend on the biofilm coverage ratio, in contrast to what is often assumed tacitly. Actually, high current density can be provided with low biofilm coverage and inversely. Experiments 8–10, which were performed with two-incubation prepared inocula, did not show coverage ratios increasing with biofilm age. The two-incubation preparation procedure had a clear effect on the kinetics of the electrochemical response but did not allow reproducible biofilm structure coverage to be obtained. Finally, the dispersion of the results was significantly reduced only when using the same inoculum as done in experiments 12–14. Experiment 14 was prolonged to 4 days, with fumarate added into the reactor. The coverage ratio obtained after 4 days indicated that the biofilm continued to grow without increasing the value of the current provided by the electrode (13.1% coverage at day 11 gave 9 A/m^2 while 13 or 14 A/m^2 were reached at day 7 with smaller coverage ratios). The biofilm age significantly affected the electrochemical efficiency of the cells. This effect may be due either to a decrease of the electrochemical efficiency of the cells themselves or to a modification (thickening for example) of the biofilm structure. It should be noted that even with the same inoculum in strictly parallel experiments with the same electrode material, biofilms of the same age can still exhibit slightly different coverage ratios (experiments 12 and 13). With a single inoculum, the physiological state of the cells cannot be a cause of the discrepancy, but other parameters, local hydrodynamic for instance, also act on primary cell adhesion, biofilm development. Parameters relating to biofilm structure that can affect the electrode/biofilm electrochemical efficiency must now be looked for.

Whatever can be the influence of the inoculum state and the biofilm age, the 14 experiments showed that 254SMO systematically gave higher current density (average J_{max} 14.1 ± 2.5 A/m^2) than 316L (average J_{max} 4.5 ± 2.3 A/m^2) (Table 1). On average, the coverage ratios were smaller for 254 SMO (in the range from 1 to 15%) than for 316 L (from 9 to 50%). It must be concluded that, statistically, the electron transfer from the material to the bacterial cells was more efficient with 254SMO than 316L since higher current were obtained on 254SMO, while it was less colonised. The difference in colonisation is relevant with the presence of higher contents of molybdenum in 254SMO (6% instead of 2%). Studies devoted to the formation of natural biofilms in freshwater have reported that the presence of molybdenum in stainless steels is detrimental to the colonisation of the surface by biofilms [27], because molybdenum affects the growth rate of the pioneering bacteria [28]. The experiments performed in parallel (no. 11–14) confirmed the strong effect of the nature of the stainless steel on the current density, with J_{max} values around 4 A/m^2 and 12 A/m^2 on 316L and 254SMO respectively. The average coverage ratios θ_A measured after 7 days of polarisation were of the same order for experiment no. 12 and 13, and even slightly higher for 316L (no. 11), which gave the smallest values of current density. In this experimental series each reactor was inoculated with the same bacterial culture, the bacterial cells expressed consequently the same electrochemical efficiency and the discrepancy in current densities can consequently be linked to the material characteristics only.

3.3. Cyclic voltammetry

Cyclic voltammetries (CVs) were performed at the beginning (before inoculation) and at the end of the experiment. Representative current–potential graphs are reported in Fig. 4. No current was observed in the control CVs recorded before the medium was inoculated with bacteria, and clear cathodic and anodic signals were

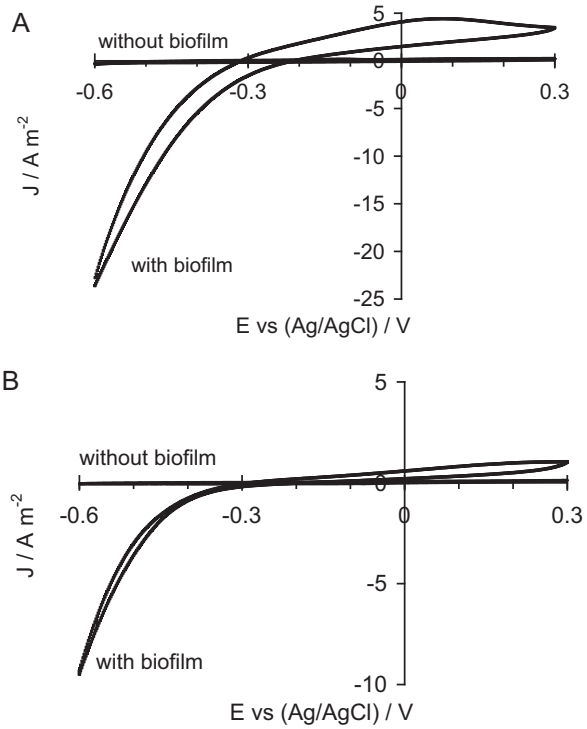

Fig. 4. Current density–potential curves on 254SMO (A: experiment 12) and 316L (B: experiment 11) at the beginning (without biofilm) and at the end of the experiment (with biofilm). CVs carried out at 10 mV/s.

recorded in the presence of the biofilm. In the anodic domain, a flat peak was observed at around 0.1 V (J_{max} = 4.1 A/m^2) on 254SMO; a small current, less than 1 A/m^2, was also observed on 316L. In contrast, no anodic current was observed during chronoamperometry at positive potential. The anodic peak was a transient phenomenon that appeared only in CVs.

In the cathodic domain (approximately at potential lower than −0.3 V vs. Ag/AgCl), the exponential shape of the current corresponded to an electrochemical kinetic controlled by electron transfer rate. Current was always higher with 254SMO electrodes than with 316L, confirming higher electron transfer rate on 254SMO. Currents recorded by CV were higher than the currents measured during chronoamperometry (Figs. 2). This difference cannot be attributed to a capacitive effect, because CVs did not show a significant hysterisis shape that characterises capacitive currents. Higher values of current are commonly obtained with high speed voltammetry compared to chronoamperometry, because high electron transfer rates are reached in CV before the substrate is depleted in the vicinity of the electrode surface. In such cases CV curves exhibit complex shapes, including current peaks that are controlled by the balance between diffusion rate and electron transfer rate. This was not the case here on the reduction side, because CV curves showed an exponential shape that indicates rate-control by pure electron transfer kinetics.

Actually, both the higher values of the reduction currents and the occurrence of an anodic peak on CV curves indicated that CV addressed a different phenomenon than chronoamperometry. Studies dealing with the catalysis of acetate oxidation by *G. sulfurreducens* biofilms have led to the same conclusion [29]. Two electrochemical steps have been distinguished with different timescale. CV detects fast electron exchange with the redox system of the adhered cells, which act as an electron storage system (step 1). Then the metabolism of the cell uses the oxidized redox compounds to oxidize acetate (step 2), this second step is controlled by

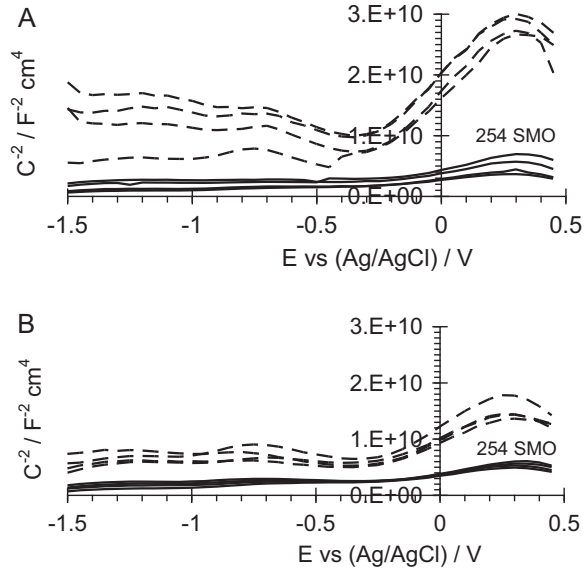

Fig. 5. Mott–Schottky diagrams on 316L and 254SMO immersed in the reactor medium before (A) and after (B) 56 h of polarisation at −0.6 V vs. Ag/AgCl.

the metabolic pathways.

$$\underset{\text{step 1 (fast)}}{\text{Cyt}_{Red} \;<=======>\; \text{Cyt}_{ox}} \;\underset{\text{step 2 (slow)}}{<- - - - - - -\; \text{Acetate}} \qquad (2)$$

This electrochemical model has been strengthened by the discovery of an abundance of c-type cytochromes in the periplasm and outer membrane of *Geobacter* species that can serve for electron storage [30,31]. Here a similar electrochemical model can be applied to fumarate reduction:

$$\underset{}{\text{Fumarate}} \;\underset{\text{step 2 (fast)}}{<----------\; \text{Cyt}_{Red}} \;\underset{\text{step 1 (fast)}}{<=========>\; \text{Cyt}_{Ox}} \qquad (3)$$

Step 1 is again a fast electron exchange with the electrode and, in the case of fumarate reduction, the metabolic reaction step 2 must be assumed to be a fast process. According to this scheme the cathodic current in CVs results from the sum of fumarate reduction and reduction of the cytochrome equipment of the cell. CVs give thus higher current than chronoamperometries, which correspond to step 2 only. The current on the oxidation branch of CVs correspond to step 1 only, because there is no compound in solution that can oxidize.

3.4. Mott–Schottky results

Mott–Schottky diagrams were recorded with 316L and 254SMO in culture medium in the absence of bacteria and under N_2/CO_2 flushing, just after immersion of the electrodes and after 56 h of polarisation at −0.6 V vs. Ag/AgCl. The reproducibility and the repeatability of profiles were checked by performing measurements twice on each of two samples of each material (Fig. 5). Flat band potentials (U_{fb}) were initially −0.29 V vs. Ag/AgCl for 316L and −0.19 V for 254SMO and they did not vary significantly after 56 h of polarisation (Table 2). The values measured here in anaerobic conditions were in the same range as values reported in the literature for aerobic media (Table 2). Results reported previously have shown strong dependence of the flat band potentials on the composition of the medium: U_{fb} of 304L has been reported at −0.49 V/SCE in artificial seawater and −0.26 V/SCE when this artificial seawater was supplemented with glucose and glucose oxidase. For 254SMO,

Table 2
Donor (N_d) and acceptor (N_a) concentrations in the passive films of 316L and 254SMO in the reactor medium, before polarisation (BP) and after 56 h of polarisation at −0.6 V vs. Ag/AgCl (AP).

Materials	Conditions		U_{fb}[a] (V)	N_a ($\times 10^{20}$ cm^{-3})	N_d ($\times 10^{20}$ cm^{-3})	W[b] (nm)
This work	254SMO	BP	−0.19[c]	[g]	19 ± 7	0.8
	254SMO	AP	−0.19[c]	[g]	16 ± 0.1	0.8
	316L	BP	−0.29[c]	8.8 ± 1	2.7 ± 0.3	1.8
	316L	AP	−0.27[c]	20 ± 6	6 ± 2	1.3
Marconnet et al. [24][e]	304L	NaCl	−0.49[d]	1.0[f]	0.25	2.15
	304L	GOx	−0.26[d]	2.9[f]	1.1	1.1
	254SMO	NaCl	−0.39[d]	[g]	0.17	2.2
	254SMO	GOx	−0.21[d]	[g]	0.93	1.43
Faimali et al. [23]	254SMO	Seawater	−0.5[c]	7.8	3.5[f]	1.21[f]

[a] The standard deviation is around 0.04 for data presented in this work.
[b] The standard deviation is less than 0.1 for data presented in this work.
[c] The values of potential are measured versus. Ag/AgCl.
[d] The values of potential are measured versus. SCE.
[e] NaCl: 0.3 g L^{-1}; GOx: 100 U L^{-1} of glucose oxidase and 20 mM D-glucose.
[f] Calculated from curves presented in the corresponding publication.
[g] Cannot be calculated since the behaviour of material is close to a conductor.

U_{fb} has been measured from −0.21 V/SCE in the same artificial seawater medium [24] to −0.5 V vs. Ag/AgCl in natural seawater [23]. Despite these variations in U_{fb} values, the stainless steels tested have always behaved like n-type semi-conductors for potentials higher than U_{fb}. Identical n-type behaviour was observed here for potentials higher than U_{fb}. The electron donor density (N_d) was initially around 2.7×10^{20} cm^{-3} and increased to 6×10^{20} cm^{-3} after 56 h of polarisation for 316L stainless steel. N_d remained almost stable for 254SMO (Table 2). These values are similar to those reported in the literature in aerobic conditions [23,24,31]. The n-type semi-conducting behaviour has been attributed to the outer part of the passive film, mainly composed of iron oxides, the contribution of chromium oxides being assumed to be negligible [32].

For potentials lower than U_{fb}, 316L showed weak p-type semi-conductive behaviour whereas 254SMO did not show any semi-conductive behaviour. A similar difference was observed between 304L and 254SMO in aerobic conditions for electrodes left at free potential [24]. After 56 h of polarisation, the acceptor density (N_a) of 316L had increased from 8.8×10^{20} to 20×10^{20} cm^{-3}. A similar p-type behaviour reported on 304L and Fe–Cr alloys in the literature has been attributed to the chromium oxide situated in the inner part of the passive film; increasing the chromium concentration increased the p-type characteristics [32]. The contribution of the outer iron oxide part of the film has been assumed negligible. 316L and 254SMO steels are characterised by relatively high amounts of chromium and nickel. Their difference in resistance to corrosion is mainly due to the difference in molybdenum content, 2% and 6% respectively. Here the absence of p-type behaviour of 254SMO may be due to the higher molybdenum content, which is known to affect the composition of the inner chromium oxide layers [33].

The *G. sulfurreducens* biofilms were grown at potentials lower than U_{fb}, at which 316L had slight p-type semi-conducting behaviour and 254SMO had no p-type behaviour. The p-type behaviour indicates a lack of available electrons close to the surface, which is obviously detrimental for a cathodic process. Moreover, the number of electron acceptors in the oxide layer, N_a, increased during polarisation. The lower efficiency observed with 316L than with 254SMO can consequently be attributed to limitation of the electronic conduction through the oxide layer of 316L. If the better performance levels of 254SMO were due to the higher molybdenum content, as suggested here, the molybdenum content of the passive layer should become a key parameter of the suitability of stainless steels to design microbial cathodes. As suggested elsewhere and also observed here, the presence of molybdenum in the passive layer has been suspected to disfavour microbial colonisation. The importance of such possible antagonist effects deserves further investigation.

4. Conclusions

The electrochemical performances of the *Geobacter sulfurreducens* biofilms revealed very sensitive to the inoculum. Preparing the inoculum with two successive incubations and performing experiments in parallel with the same inoculum significantly improved the reproducibility of the electrochemical results. Such well controlled conditions confirmed that the maximum current density is not straightforwardly correlated to biofilm coverage ratios.

254SMO superaustenitic steel led to more efficient biocathodes than 316L austenitic steel. This difference was not correlated with differences in bacterial settlement on the material surface. In contrast, the materials showed a clear difference in their semi-conductive behaviour at the potential value used here for chronoamperometry. Stainless steels were confirmed to be excellent materials for building microbial cathodes and efforts to improve microbial cathodes must now take the conductive and semi-conductive properties of the oxide layer of steels into consideration. Incidentally, the low biofilm coverage ratio observed, less than 10%, gives hope that current densities can still be drastically improved by increasing the biofilm coverage.

Acknowledgements

The authors are grateful to Dr. Damien Féron (CEA-Saclay, France) for numerous helpful discussions and Luc Etcheverry (CNRS engineer, Laboratoire de Génie Chimique) for his efficient help.

References

[1] L.M. Tender, C.E. Reimers, H.A. Stecher, D.E. Holmes, D.R. Bond, D.A. Lowy, K. Pilobello, S.J. Fertig, D.R. Lovley, Nat. Biotechnol. 20 (2002) 821.
[2] D.R. Bond, D.E. Holmes, L.M. Tender, D.R. Lovley, Science 295 (2002) 483.
[3] B.E. Logan, J.M. Regan, Trends Microbiol. 14 (2006) 512.
[4] Z. Du, H. Li, T. Gu, Biotechnol. Adv. 25 (2007) 464.
[5] D.R. Lovley, Curr. Opin. Biotechnol. 19 (2008) 564.
[6] T.H. Pham, P. Aelterman, W. Verstraete, Trends Biotechnol. 27 (2009) 168.
[7] A. Bergel, D. Féron, A. Mollica, Electrochem. Commun. 7 (2005) 900.
[8] C. Dumas, A. Mollica, D. Féron, R. Basseguy, L. Etcheverry, A. Bergel, Electrochim. Acta 53 (2007) 468.
[9] Z. He, L.T. Angenent, Electroanalysis 18 (2006) 2009.
[10] J.M. Tront, J.D. Fortner, M. Plötze, J.B. Hughes, A.M. Puzrin, Biosens. Bioelectron. 24 (2008) 586.
[11] S.M. Strycharz, T.L. Woodward, J.P. Johnson, K.P. Nevin, R.A. Sanford, F.E. Loeffler, D.R. Lovley, Appl. Environ. Microbiol. 74 (2008) 5943.
[12] F. Aulenta, A. Canosa, P. Reale, S. Rossetti, S. Panero, M. Majone, Biotechnol. Bioeng. 103 (2009) 85.
[13] H. Liu, B. Logan, Environ. Sci. Technol. 39 (2005) 4317.

[14] R.A. Rozendal, H.V.M. Hamelers, G.J.W. Euveriknk, S.J. Metz, C.J.N. Buisman, Int. J. Hydrogen Energy 31 (2006) 1632.
[15] B.E. Logan, D. Call, S. Cheng, H.V.M. Hamelers, T.H.J.A. Sleutels, A.W. Jeremiasse, R.A. Rozendal, Environ. Sci. Technol. 42 (2008) 8630.
[16] D. Call, B. Logan, Environ. Sci. Technol. 42 (2008) 3401.
[17] R.A. Rozendal, A.W. Jeremiasse, H.V.M. Hamelers, Environ. Sci. Technol. 42 (2008) 629.
[18] K.B. Gregory, D.R. Bond, D.R. Lovley, Environ. Microbiol. 6 (2004) 596.
[19] C. Dumas, R. Basseguy, A. Bergel, Electrochim. Acta 53 (2008) 2494.
[20] R. Devaux-Basseguy, A. Bergel, M. Comtat, Enz. Microbial. Technol. 20 (1997) 248.
[21] T.R. Garrett, M. Bhakoo, Z. Zhang, Prog. Nat. Sci. 12 (2008) 1049.
[22] D.A. Shifler, Corros. Sci. 47 (2005) 2335.
[23] M. Faimali, E. Chelossi, F. Garaventa, C. Corra, G. Greco, A. Molllica, Electrochim. Acta 54 (2008) 148.
[24] C. Marconnet, Y. Wouters, F. Miserque, C. Dagbert, J.P. Petit, A. Galerie, D. Feron, Electrochim. Acta 54 (2008) 123.
[25] S. Dulon, S. Parot, M.L. Delia, A. Bergel, J. Appl. Electrochem. 37 (2007) 173.
[26] A. Larrosa, L.J. Lozano, K.P. Katuri, I. Head, K. Scott, C. Godinez, Fuel 88 (2009) 1852.
[27] J. Kielemoes, F. Hammes, W. Verstraete, Environ. Technol. 21 (2000) 831.
[28] S.L. Percival, J. Ind. Microbiol. Biotechnol. 23 (1999) 112.
[29] C. Dumas, R. Basseguy, A. Bergel, Electrochim. Acta 53 (2008) 5235.
[30] A. Esteve-Nunez, J. Sosnik, P. Visconti, D.R. Lovley, Environ. Microbiol. 10 (2008) 497.
[31] D.R. Lovley, Geobiology 6 (2008) 225.
[32] N.E. Hakiki, S. Boudin, B. Rondot, D. Da Cunha Belo, Corr. Sci. 37 (1995) 1809.
[33] M.F. Montemeor, A.M.P. Simoes, M.G.S. Ferreira, M. Da Cunha Belo, Corr. Sci. 41 (1999) 17.